Optical absorption spectra of tourmaline crystals from Altay, China

Xueliang Liu (刘学良)[1*], Xiqi Feng (冯锡琪)[2], Jianliang Fan (范健良)[1], and Shouguo Guo (郭守国)[1]

[1] *Gemstone Testing Center, East China University of Science and Technology, Shanghai 200237, China*

[2] *Shanghai Institute of Ceramics, Chinese Academy of Sciences, Shanghai 200050, China*

[*] *Corresponding author: xlliu@ecust.edu.cn*

Received February 17, 2011; accepted March 15, 2011; posted online June 21, 2011

Tourmaline is an important functional and gem material. The current study examines pink, green, and brownish-green tourmalines from Altay deposit. Based on X-ray fluorescence (XRF) quantitative analyses and ultrariolet-visible-near-infrared (UV–VIS–NIR) spectral analyses in combination with annealing experiments, the color center of tourmaline is found to be related to the $d-d$ transitions of ions or the $d-d$ transitions of exchange coupled ions. Annealing treatment affects the color improvement of tourmaline crystals.

OCIS codes: 300.6170, 160.2710.

doi: 10.3788/COL201109.083001.

Tourmaline is a type of borate-silicate mineral with an extremely complex chemical component and crystal structure. Its crystal-chemical behavior, physical property, and origin have attracted substantial attention in the fields of materials science and physics[1−3]. Tourmaline displays a unique range of colors and is frequently used as a gem[4]. However, research on tourmaline is limited. For instance, knowledge about the color centers in different species of tourmaline remains very poor. As a result, its further development and application are largely limited[5].

The general formula of the tourmaline group of minerals is XY_3Z_6 (T_6O_{18}) $(BO_3)_3V_3W$[4−10]. In this formula, X sites are occupied by alkaline ions and vacancies; Y sites are mainly occupied by Mg^{2+}, Fe^{2+}, and Mn^{2+}, among others, which are expressed as M_Y ions in the current letter; Z sites are primarily occupied by trivalent ions of smaller size such as Al^{3+}, Fe^{3+}, Cr^{3+}, and V^{3+}. A minor amount of other ions such as Mg^{2+} and Fe^2 can also be found in these sites. Similarly, the metallic ion at the Z site is expressed as M_Z. T sites are mainly occupied by Si^{4+} and corner-sharing tetrahedra (T sites) form hexagonal rings. V sites are mainly occupied by OH^- and O^{2-}. W sites are occupied by O^{2-}, OH^-, and F^-.

Black tourmaline is common in the hundreds of thousands of granite-pegmatite veins found in Altay, China. The colorful tourmaline rarely shows[11]. However, knowledge about the chemical structure, color center, and gem treatment of its different species remains limited[12−15]. In this letter, representative pink, green, and brownish-green tourmalines from Altay are selected as the research objects.

Three different species are highly idiomorphic single crystals. Sample 1, is a two-color tourmaline. However, all subsequent tests and analyses are based on its pink side. Sample 2 is a type of gem-grade green tourmaline crystal. Sample 3 is of dark black color and has poor transparency perpendicular to the c-axis. It has a brownish-green color and relative better transparency parallel to the c-axis. Along the direction perpendicular to the c-axis, three tourmaline crystals are cut into slices about 1 mm in thickness; these slices are polished at both sides.

Quantitative analyses of the tourmaline samples are conducted using X-ray fluorescence (XRF) spectrometer (XRF-1800, Shimadzu Japan) sequential XRF. The parameters used are as follows: power of 40 kV, current of 95 mA, scanning speed of 8°/min, and target Rh and detectable element range of ^{8}O–^{92}U. The analytic results are expressed as oxide content.

The UV–VIS–NIR optical absorption spectra of the tourmalines samples are obtained using a spectrophotometer (Cary 500, Agilent, USA).

Annealing experiments of the tourmaline samples are performed in a furnace with a temperature error within ±5 °C. For each experiment, the heating rate is 5 °C/min, and the cooling down rate is 3 °C/min. In our experiments, the first type of heat treatment performed at 700 °C in air for 3 h was conducted on samples 1, 2, and 3, and the second type of heat treatment performed at 750 °C in air for 3 h was conducted on sample 3.

The quantitative analytical results of three samples are obtained by XRF. However, some light elements cannot be detected. Considering the main components, the structural formula of samples 1, 2, and 3 can be simplified as XY_3Z_6 $(Si_6O_{18})(BO_3)_3(OH)_3(O, OH)$. Reasonable quantitative analytical results (shown in Table 1) are obtained. Similar quantitative analyses of tourmalines from Altay have been reported by Wang *et al.*[14,15]. Their findings match, and the samples selected in the present study are found to be representative as well.

The color centers of natural tourmalines are commonly known to be related to the existence of manganese (Mn^{2+}, Mn^{3+}), iron (Fe^{2+}, Fe^{3+}), and titanium (Ti^{4+}). The pink color is related to the presence of manganese, whereas the green color is related to the presence of iron[4]. According to Table 1, the pink color of sample 1 is related to the presence of manganese, the green color of sample 2 is related to the presence of manganese and iron, and the brownish-green color of sample 3 may be

Table 1. Chemical Components and Contents (wt.-%) of Samples 1, 2, and 3

Sample	1	2	3
SiO_2	38.54	37.73	39.06
Al_2O_3	39.95	41.06	36.04
$Fe_2O_3^a$	ND	4.24	3.30
MnO^b	0.09	0.61	2.23
Na_2O	1.42	ND	2.14
TiO_2	ND	ND	0.32
MgO	ND	ND	0.31
CaO	2.62	0.56	0.30
CuO	ND	ND	0.18
PbO	1.41	0.07	0.03
Ga_2O_3	0.10	0.04	0.03
Cr_2O_3	ND	ND	0.02
ZnO	ND	0.11	0.02
Co_2O_3	ND	0.04	0.02
K_2O	ND	0.09	ND
B_2O_3	11.24	11.01	11.39
OH^-+O^{2-}	4.55	4.45	4.61
Total	100.00	100.00	100.00

a: total content of Fe element, including Fe^{2+} and Fe^{3+}; b: total content of Mn element, including Mn^{2+}, Mn^{3+}, and Mn^{4+}; ND: not detected

(a) (b)

Fig. 1. (Color online) (a) Pink color of sample 1 changed to (b) colorless after annealing at 700 °C in air for 3 h.

related to the presence of not only manganese and iron but also of other metallic ions such as Ti^{4+}, Cu^{2+}, Co^{2+}, Co^{3+}, and Cr^{3+}.

After annealing at 700 °C in air for 3 h on three different species of the tourmaline samples, the pink color of sample 1 changed to colorless (Fig. 1), whereas the colors of samples 2 and 3 showed no change. Combined with the analyses of transition metallic ions in sample 1, the disappearance of the pink color is evidently related to the oxidation of manganese ion (Mn^{2+}, Mn^{3+}). After annealing at 750 °C in air for 3 h, sample 3 showed a more intense brown color and great amounts of parallel fractures in the surface as shown in Fig. 2(d). The formation of of parallel fractures is considered a structural adjustment of the tourmaline crystal[4].

The optical absorption spectra ($E//c$) of sample 1 (pink) in the range of 300–800 nm are shown in Fig. 3. The original spectrum has four small bands at 357, 452, 540, and 618 nm, as well as two broad, more intense bands at 392 and 517 nm. After annealing, the bands at 392 and 517 nm completely disappear, whereas other small bands show no obvious change. Obviously, the origins of the bands at 392 and 517 nm, which lead to the appearance of the pink color, are different from that

(a) (b) (c) (d)

Fig. 2. (Color online) Changes in sample 3 after annealing at a high temperature in air for 3 h (a–untreated; b–700 °C; c–750 °C). Sample 3 has an evidently more intense brown color and exhibits great amounts of parallel fractures in the surface (as shown in Fig. 2(d), observation under 50× microscopy) after annealing.

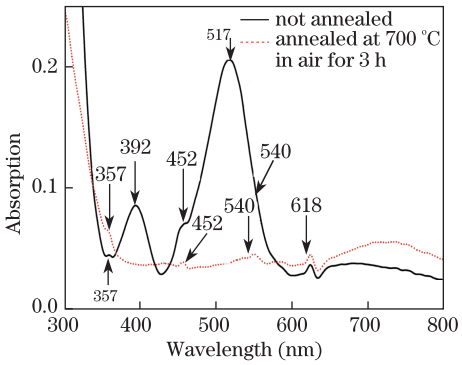

Fig. 3. Spectral changes in sample 1 in the range of 300–800 nm after annealing at 700 °C in air for 3 h.

of other bands.

The bands at 392 and 517 nm have been related to the presence of Mn^{3+}, and have been considered the $d-d$ transitions ($^5E_g \rightarrow {}^5T_{2g}$) of Mn^{3+} at Y octahedral sites[9,10,16–18]. The spectroscopic features of Mn^{2+} are easily recognized by their narrow, weak absorption bands between 410 and 420 nm[10,17], whereas they cannot be observed in the optical absorption spectra of sample 1. Therefore, the main occurrence valence state of the manganese ion in sample 1 is confirmed to be +3 and/or +4 rather than +2. Due to the lack of $3d$ electron, a single Mn^{4+} has no contribution to absorption and to the color of tourmaline. For trivalent manganese (Mn^{3+}) located at the Y octahedral site in tourmaline crystal, it is affected by the crystal field of oxygen octahedron. Therefore, the d electron splits into three T_g orbits of a lower energy level and two E_g orbits of a higher energy level. The high-spin $3d^4$ electron cloud of Mn^{3+} results in an uneven possession of the E_g energy level, which leads to octahedral distortion and the Jahn-Teller effect. Accordingly, the pink color of tourmaline originates from the $d-d$ transitions ($^5E_g \rightarrow {}^5T_{2g}$) of Mn^{3+} at Y sites, which lead to the bands at 392 and 517 nm in the visible light range. However, Mn^{3+} can easily be oxidized to the more stable Mn^{4+} when heat-treated at a high temperature in air.

The optical absorption spectra (E//c) of sample 2 (green) before and after annealing in air for 3 h are shown in Fig. 4. There is no obvious spectral change in the range of 300–1 400 nm after annealing, and intense bands near 420, 718, and 1 150 nm coupled with one weak band near 618 nm are observed in both spectra. The bands (392, 517 nm) that originate from the $d-d$ transitions of Mn^{3+} would disappear when heat-treated at 700 °C in air (Fig. 4). Therefore, the main occurrence valence state of manganese in sample 2 is +2 and/or +4 rather than +3. The optical absorption spectra (E//c) of the sample

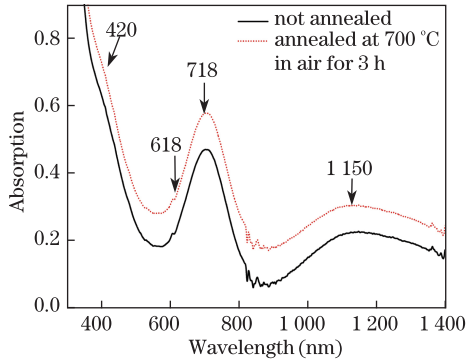

Fig. 4. Spectral changes in sample 2 in the range of 350–1 400 nm after annealing at 700 °C in air for 3 h.

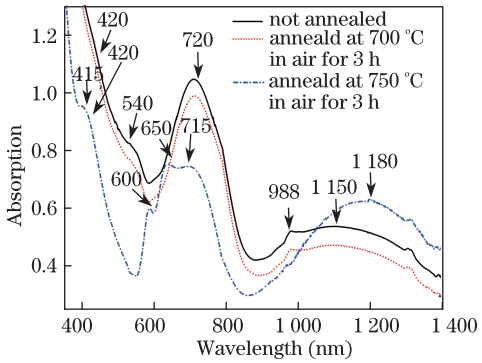

Fig. 5. Spectral changes in sample 3 in the range of 350–1 400 nm after annealing at 700 and 750 °C in air for 3 h.

(brownish-green) in the range of 350−1 400 nm are shown in Fig. 5. There is no obvious difference between the spectra before and after annealing at 700 °C in air, and four broad bands near 420, 540, 720, and 1 150 nm coupled with one weak band near 988 nm are observed in both spectra. For the effects of annealing at 750 °C in air for 3 h on tourmaline 3, absorption near 540, 720, and 988 nm is obviously weakened; absorption near 415, 600, and 650 nm is strengthened; and the band at 1 150 nm that red-shifts to the long wavelength end (maximum at 1 180 nm) with absorption is strengthened. Obviously, the bands near 540, 720, and 1 150 nm are related to Fe^{2+}, whereas the bands at 415, 420, 600, 650, 988, and 1 180 nm are related to Fe^{3+}. Additionally, Fe^{2+} is oxidized to Fe^{3+} when heat-treated at 750 °C in air.

The vibrations related to the –OH groups are important in examining the crystal structure of tourmaline. The optical absorption spectra (E//c) of samples 1, 2, and 3 in the NIR range of 4 800–4 000 cm^{-1} before and after annealing are shown in Fig. 6. A group of weak, sharp bands are observed in each spectrum, and these bands show no change after annealing at 700 °C. The optical absorption spectra (in the near-infrared range) of the pink and green tourmalines from Brazil have been discussed by Reddy, who assigned the bands in this range to the combination of the stretching and bending modes of cationic hydroxyl units (M–OH)[10,20]. The absorption bands of the three present samples and two samples from Reddy are discussed in Table 2.

For M_Y–$OH_{(1)}$ units, the combination of the stretching and bending modes commonly leads to three bands in the range of 4 700–4 400 cm^{-1}. Although, the chemical components of the five samples are significantly different,

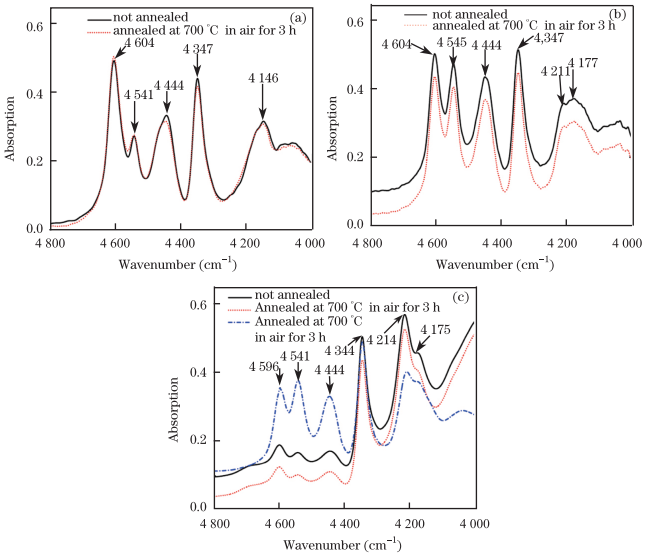

Fig. 6. Spectral changes in the samples in the range of 4,800–4,000 cm^{-1} after annealing in air for 3 h, (a) sample 1; (b) sample 2; (c) sample 3.

Table 2. Absorption Bands (cm^{-1}) of Samples 1, 2, and 3 in the Range of 4 800–4 000 cm^{-1} and Their Respective Assignments

In this letter			Reddy[19]		Assignments	
Pink 1	Green 2	Brownish -Green 3	Pink	Green		
4 146	4 177	4 175		4 171	Combination	M_Y–$OH_{(3)}$
	4 211	4 214	4 194		of Stretching	M_Y–$OH_{(3)}$
4 347	4 347	4 344	4 340	4 347	and Bending	M_Z–$OH_{(3)}$
4 444	4 448	4 444	4 433	4 433	Modes of M–	M_Y–$OH_{(1)}$
4 541	4 545	4 541	4 535	4 538	OH Units	M_Y–$OH_{(1)}$
4 604	4 604	4 596	4 601	4 597		M_Y–$OH_{(1)}$

especially in terms of metallic ions at Y sites, the resulting bands show much approximate peak values, which are observed near 4 600, 4 540, and 4 440 cm^{-1}. Considering the slight change for these bands after annealing at 700 or 750 °C in air for 3 h, the hydroxyl groups at W sites are evidently restricted in the crystal structure of tourmaline, and the combination bands of M_Y–$OH_{(1)}$ units are slightly affected by M_Y metallic ions. The bands at ∼4 600 cm^{-1} are considered the combination bands involving Al-OH units[10]. Therefore, the bands near 4 600 cm^{-1} are due to the combination bands involving Al_Y–$OH_{(1)}$ units.

The band in the range of 4 400–4 300 cm^{-1} is due to the combination of the stretching and bending modes of M_Z–$OH_{(3)}$ units. The Z sites in the three samples are mainly occupied by Al^{3+}. Therefore, M_Z–$OH_{(3)}$ units are mainly composed of Al_Z–$OH_{(3)}$ units, whose combination band is observed near 4 344 cm^{-1}. Al^{3+} is not a transition metallic ion, so the band due to Al_Z–$OH_{(3)}$ units did not change after annealing at 700 or 750 °C in air.

For M_Y–$OH_{(3)}$ units, the combination of stretching and bending modes commonly leads to two bands in the range of 4 300–4 100 cm^{-1}. In view of relative bands as shown in Table 2, M_Y–$OH_{(3)}$ units are much complex for

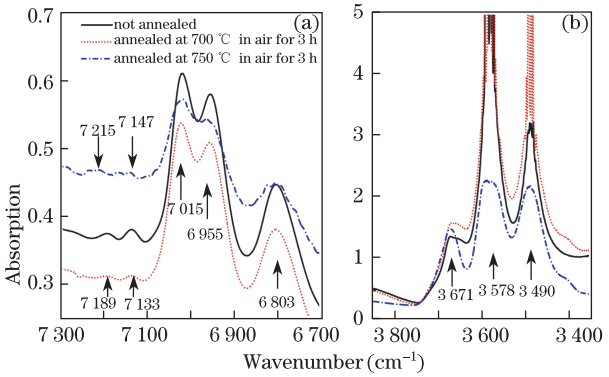

Fig. 7. Optical absorption spectra of sample 3 before and after annealing at 700 °C and 750 °C in air for 3 h. (a) Bands in the range of 7 300–6 700 cm^{-1}; (b) bands in the range of 3 850–3 350 cm^{-1}.

Table 3. Absorption Bands of Sample 3 in the NIR Region and Their Respective Assignments

Bands(cm^{-1})	Assignments	Modes
3 490	–$OH_{(3)}$–(Al, Fe, Mn)$_Y$Al$_Z$Al$_Z$	Hydroxyl Stretching
3 580	–$OH_{(3)}$–(Al, Fe, Mn)$_Y$Al$_Z$Al$_Z$	
3 670	–$OH_{(1)}$–(Al, Fe, Mn)$_Y$	
6 803	–$OH_{(3)}$–(Al, Fe, Mn)$_Y$Al$_Z$Al$_Z$	First Fundamental
6 950	–$OH_{(3)}$–(Al, Fe, Mn)$_Y$Al$_Z$Al$_Z$	Overtone of
7 017	–$OH_{(3)}$–(Al, Fe, Mn)$_Y$Al$_Z$Al$_Z$	Hydroxyl Stretching
7 132	–$OH_{(1)}$–(Al, Fe, Mn)$_Y$	
7 189	–$OH_{(1)}$–(Al, Fe, Mn)$_Y$	

many types of metallic ions located at Y sites, involving (Al, Li, Fe, Mn)$_Y$–$OH_{(3)}$ units.

Figure 7 shows the optical absorption spectra of sample 3 before and after annealing at 700 and 750 °C in air for 3 h. The spectra in the range of 3 850–3 350 cm^{-1} are shown in Fig. 7(b). Three strong bands near 3 670, 3 580, and 3 490 cm^{-1} are observed in the three spectra. These bands are considered the hydroxyl stretching modes[10,21,22]. The spectra in the range of 7 300–6 700 cm^{-1} are shown in Fig. 7(a). Five weak bands near 7 189, 7 133, 7 015, 6 955, and 6 803 cm^{-1} are observed in both spectra of the sample before and after annealing at 700 °C, whereas the bands near 7 189 and 7 133 cm^{-1} shift to 7 215 and 7 147 cm^{-1} after annealing at 750 °C. These bands are considered the first fundamental overtones of hydroxyl stretching modes[10]. Table 3 shows the absorption bands of sample 3 in the NIR region and their respective assignments. Therefore, the bands at 3 490 and 3 578 cm^{-1} are together attributed to the stretching modes of the –$OH_{(3)}$ groups, whereas the band at 3 671 cm^{-1} is due to the stretching modes of the –$OH_{(1)}$ groups. Further, the bands at 6 803, 6 955, and 7 015 cm^{-1} are due to the first fundamental overtones of the stretching modes of the –$OH_{(3)}$ groups, whereas the bands at 7 189 and 7 132 cm^{-1} are due to the first fundamental overtones of the stretching modes of the –$OH_{(1)}$ groups.

In conclusion, based on quantitative analyses by XRF, the optical absorption spectra of pink, green, and brownish-green tourmalines were subsequently discussed in combination with annealing experiments performed at 700 and 750 °C in air for 3 h. The color center of pink tourmaline is related to the $d-d$ transitions of Mn^{3+} at Y sites, which leads to two broad, intense bands at 392 and 517 nm. Mn^{3+} can easily be oxidized to a more stable Mn^{4+} so that the bands related to Mn^{3+} disappeared, and the pink color changed to colorless after annealing at 700 °C in air. Annealing treatment affects the color improvement of tourmaline crystals. The green color of tourmaline mainly depends on the intense bands near 420 and 718 nm, which were respectively considered the $d-d$ transitions of the exchange coupled Fe^{3+}–Fe^{3+} ion pairs and Fe^{2+}–Fe^{3+} ion pairs. For brownish-green tourmaline, its brown color depends on the band near 540 nm, which is considered the charge transfer of the Fe^{2+}–Ti^{4+} ion pairs. The bands in the ranges of 3 800–3 400 cm^{-1}, 7 300–6 800 cm^{-1}, and 4 800–4 000 cm^{-1} are related to hydroxyl stretching modes.

References

1. J. Zhan, X. Hao, H. Liu, B. Huang, and X. Tao, J. Functional Mater. (in Chinese) **37,** 524 (2006).
2. K. Jiang, T. Sun, L. Sun, and H. Li, J. Environmental Sci. **18,** 1221 (2006).
3. S. Yamaguchi, Appl. Phys. A **31,** 183 (1983).
4. C. Castaneda, S. G. Eeckhout, G. M. Costa, N. F. Botelho, and E. De Grave, Phys. Chem. Miner. **33,** 207 (2006).
5. M. Taran, A. Lebedev, and A. Platonov, Phys. Chem. Miner. **20,** 209 (1993).
6. F. C. Hawthorne and D. J. Henry, Eur. J. Mineral. **11,** 201 (1999).
7. E. Ferrow, Hyperfine. Interact. **91,** 689 (1994).
8. Y. Fuchs, M. Lagache, and J. Linares, Comptes. Rendus. Geosciences. **334,** 245 (2002).
9. K. Krambrock, M. Pinheiro, S. Medeiros, K. Guedes, S. Schweizer, and J. M. Spaeth, Nuclear Instru. Meth. Phys. Res. Section B **191,** 241 (2002).
10. B. J. Reddy, R. L. Frost, W. N. Martens, D. L. Wain, and J. T. Kloprogge, Vib. Spectrosc. **44,** 42 (2007).
11. G. Liu and H. Lu, China Geochemistry **5,** 234 (1986).
12. A. C. Zhang, R. C. Wang, S. Y. Jiang, H. Hu, and H. Zhang, Can. Mineral. **46,** 41 (2008).
13. J. Wang, X. Tao, and W. Wang, Acta Petrologica et Mineralogica (in Chinese) **24,** 319 (2005).
14. Y. Wang, X. Kang, S. Wang, and Y. Liao, Mineral Res. Geo. (in Chinese). **10,** 172 (1996).
15. R. Wu, S. Lin, F. Bai, and S. Zhang, Acta Petrologica et Mineralogica (in Chinese) **17,** 371 (1998).
16. P. G. Manning, Can. Mineral. **11,** 971 (1973).
17. Z. Lü, K. Zhao, H. Liu, N. Zhou, H. Zhao, and L. Gao, Chin. Opt. Lett. **7,** 718 (2009).
18. M. B. De. Camargo and S. Isotani, Am. Mineral. **73,** 172 (1988).
19. D. Cao, G. Zhao, Q. Dong, J. Chen, Y. Cheng, and Y. Ding, Chin. Opt. Lett. **8,** 303 (2010).
20. N. Garces, K. Stevens, L. Halliburton, M. Yan, N. Zaitseva, and J. DeYoreo, J. Cryst. Growth **225,** 435 (2001).
21. I. M. Reinitz and G. R. Rossman, Am. Mineral. **73,** 822 (1988).
22. D. Cao, G. Zhao, Q. Dong, J. Chen, Y. Cheng, Y. Ding, and J. Zou, Chin. Opt. Lett. **8,** 199 (2010).